

Effect of Surcharge on Arching Phenomena in Henomena in Back of MSE Walls

Suresh Kommu

¹Sr.Assistant Professor, Dept. of Civil Engineering, VNRVJIET, Hyderabad, Telangana, India
Sureshkommu.me@gmail.com

Krishna Karthika Gorla

²Master Student, Dept. of Civil Engineering, VNRVJIET, Hyderabad, Telangana, India
krishnakarthika11@gmail.com

Abstract

Back-to-Back walls are the complex geometry of MSE walls and are often used as approach embankments and bridge abutments. Surcharge loads acting on the Back to Back Mechanically Stabilized Earth Wall (BBMSEW) should be applied on BBMSE walls to understand the realistic behavior. In this study, Numerical modeling is performed with Plaxis 2D to understand the consequence of surcharge on earth pressures, surface settlement profiles of BBMSE walls. A typical ratio of $W/H=1.55$ is taken where a combination of a reinforced and unreinforced zone is present in BBMSEW for analysis and reinforcement stiffness of (J) from 50 to 50000 kN/m is used to study the flexibility of the backfill with the reinforcement within. The stress analysis at the transition plane of the reinforced and unreinforced zone showed the arching phenomena. Due to the surcharge, the lateral pressure reduced nearly 42.31% from the Rankine's active condition and the vertical stresses are very close to the analytical arching equation derived and reduced approximately 63.51% from the overburden pressure after surcharge is applied. It is found that the surface settlement profiles for a particular stiffness (i.e., $J=50000\text{kN/m}$) at different wall heights are decreasing from top to bottom. At 6m height for $J=50\text{kN/m}$, it is observed that the settlements have occurred in the reinforced zone whereas for the $J=50,000\text{kN/m}$ the settlements were observed only in the unreinforced zone. From the analysis, it is concluded that arching is predominant in the transition zone of BBMSEW and must be considered for the estimation of earth pressure and design of BBMSEW.

Keywords: Surcharge load, vertical stress, Arching, Numerical model, Back-to-back walls, Surface Settlement profile

1. Introduction

Back to Back MSE wall structures must be designed to ensure that they are stable externally and internally. Compound global stability analysis must be ensured to build a safe BBMSEW. The schematic of BBMSEW is shown in Fig.1. The design principles of this complex geometry of MSE Wall are given in the codes. However, the design principles presented in the codes are limited and must be analyzed carefully to design the BBMSEW.

In the designing of the wall, the three controlling factors include the geometry of the wall, stresses acting, and the deformations of BBMSEW. The stability analysis of the wall if $W/H < 2$ is not mentioned in the codes and has limited study. If $W/H < 2$, the stresses acting at the transition plane of reinforced and unreinforced zone is overestimated which leads to the unsafe design of the wall and further leads to failure of the structure. In the present study the stresses acting at the transition plane of the reinforced and unreinforced zone of BBMEW is analyzed using the numerical model simulated in Plaxis 2D. Two factors which contribute the stability of the structure are: one is the reinforcement providing enough tensile strength and the other is the soil having shear strength.

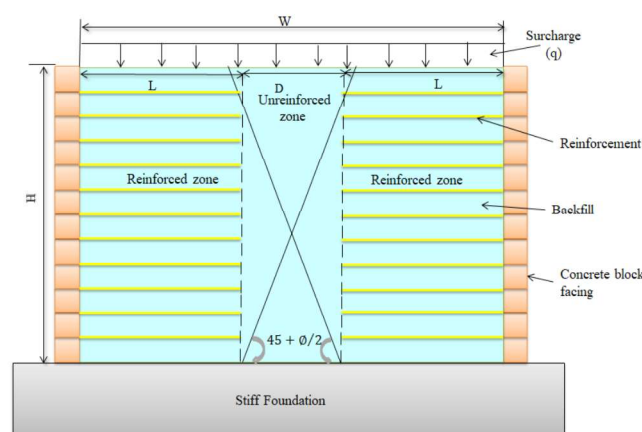


Fig.1. Schematic of BBMSEW (Back to Back Mechanically Stabilized Earth Wall).

Modeling of BBMSEW were dealt in studies developed a wide variety of numerical models using the methods of finite element and finite difference software and validated with field instrumented studies and analyzed the earth pressures, lateral displacements, and settlements of the walls. And the consequence of surcharge on single MSE walls, the studies in BBMSEW surcharge induced effect on BBMSEW. In the BBMSEW there are two zones as shown in Fig.1. Reinforced and unreinforced zone as from the basic principle arching is the process by which stresses are transferred from the soil on to adjacent structure due to

mobilization of shear stresses resulting from relative displacements. Where the relative displacements are observed in the BBMSEW due to the rigidity difference between the reinforced and unreinforced zone in which the studies are on various geotechnical structures like buried structures, embankments, silos, mine stopes and retaining walls.

A detailed study on Back to Back MSE walls, arching, and the consequence of surcharge on arching suggests that the studies are limited in BBMSEW. The main intention of this study is to analyze the phenomenon of arching under controlled conditions assuming the wall is rotated about the top by applying K_a condition on the exterior of the wall, for limit state analysis and surcharge application on the BBMSEW. In this study earth pressures in the lateral and vertical direction, values of settlements necessary to mobilize arching in the transition plane of BBMSEW, and the extent of the zone of stress transfer are analyzed and presented.

2. Numerical Modeling

A numerical model was simulated as shown in Fig.2. Wall height (H) is 6 m, with a vertical facing. The length of geogrid reinforcement was 0.7H i.e. 4.2m as prescribed in the codes, and the minimum spacing specified in codes is 0.6m between the reinforcement respectively. The input parameters for this soil model and reinforcement were presented in Table 1. & Table 2. For the soil Mohr-Coulomb model, i.e., a linear elastic and perfectly plastic was applied. Reinforcement of geogrid is modeled as elastic material which is perfectly compatible with the soil in the model. The interfaces are created for soil-block, having soil properties with interface friction ($R_{inter}=0.8$), and for a block-block interface is created using concrete block properties using interface friction ($R_{inter}=0.8$) and soil-reinforcement to ensure the friction between the elements and are compatible with the soil element.

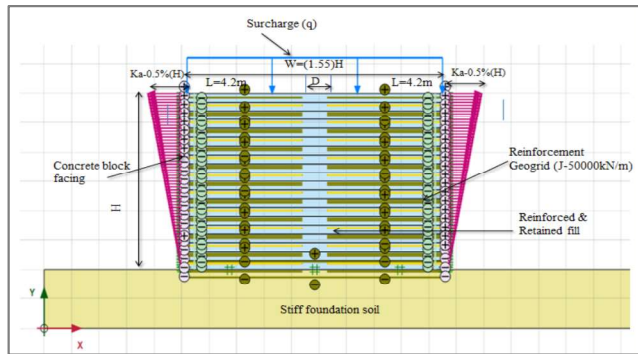


Fig.2 Numerical model of BBMSEW in Plaxis 2D

Staged construction is simulated with each layer of 0.3m thickness was placed till the wall height of 6m is constructed. And the surcharge (q) of 24kPa is kept on the top of BBMSEW after construction to simulate the dead load and live load acting on the wall as per codes. The boundary was fixed both in a horizontal and vertical direction from the base of the wall in between the facings of the wall above the foundation to not allow the settlement from the wall to the foundation. K_a condition was imposed with a prescribed lateral displacement of 0.03m (i.e., 0.5%H) and vertical displacement is fixed on facing of the wall, Across the wall height with uniformly varying to perform the limit state analysis as shown in Fig.2. The analysis is

performed for the lateral earth pressures, vertical stresses, and the surface settlement profiles were taken and compared with the analytical equation derived and shows satisfactory concurrence between the obtained and intended values of the horizontal and vertical stresses after construction. And also the comparison of the lateral and vertical stresses, the surface settlement profiles with and without surcharge of BBMSEW is analyzed and presented. And to understand the flexibility behavior of the backfill within the wall, stiffness of the reinforcement is varied from $J=50$ kN/m to 50,000 kN/m, vertical stresses and surface settlement profiles were taken and presented.

Table1: Soil and concrete block properties of numerical model

Properties	Backfill	Foundation soil	Concrete block
Soil model	Mohr-coulomb	Mohr-coulomb	Linear elastic
Unit weight $\gamma(kN/m^3)$	20	22	24
Elastic modulus (E)kPa	30E3	2E6	30E6
Poisson's ratio (ν)	0.3	0.2	0.15
Cohesion(c) kPa	2	1000	-
The angle of shearing resistance(ϕ) degrees	35	50	-
Dilation (ψ) 'degrees	11	0	-

Table2: Geogrid reinforcement properties

Properties	Stiffness(J) kN/m
Geogrid reinforcement	50,500,5000,50000

3. Validation of model

For the validation of the present study, the same configuration was taken by [11] as shown in Fig.3, is simulated using Plaxis 2D. The Wall height is 6 m, and the depth of the foundation is 2 m. Here, 2 cases are considered ($W/H=2$ and $W/H=1.4$) and a concrete block facing is used to simulate the field condition, the concrete blocks with a dimension of 0.3x0.2m are used as facing for the BBMSEW. The connection between the reinforcement and modular concrete block is fully fixed and there is no error in the connection is ensured. The interface is generated between block-block, soil-reinforcement, block-soil, and at the base between the foundation and above backfill.

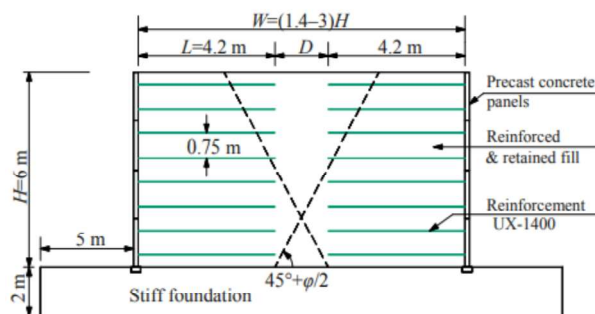


Fig.3. Schematic of BBMSEW model for validation

The properties of the backfill, concrete blocks, reinforcement which are given as the input parameters to the Plaxis for validation are presented in Table 3. and Table 4.

Table 3 Backfill and foundation soil properties for validation

Properties	Infill	Base soil
Soil model	Mohr-coulomb	Mohr-coulomb
Unitweight $\gamma(kN/m^3)$	18	22
Elastic modulus (E)kPa	30E3	200E3
Poisson's ratio(ν)	0.3	0.2
Cohesion(c) kPa	0	100
The angle of shearing resistance(ϕ) degrees	30,35,40	30
Dilation (ψ) degrees	5	0

Table 4 Reinforcement properties for validation

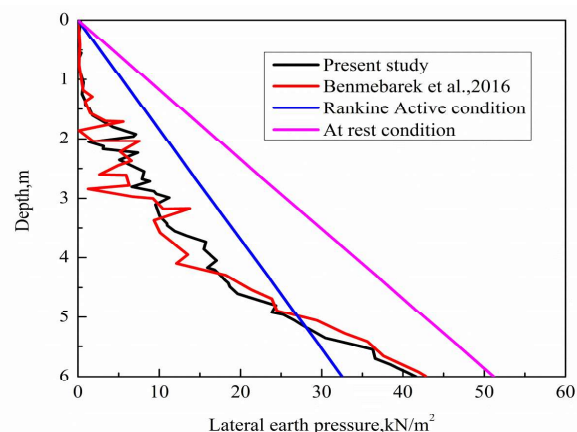
Properties	Stiffness(J) kN/m
Geogrid reinforcement	11000

However, in the present study reinforcement stiffness is taken from $J=50$ to $50,000$ kN/m. But the model with the stiffness of $J=50,000$ kN/m is compared with the validation results. And a vertical spacing of 0.75 m is used for reinforcement in backfill.

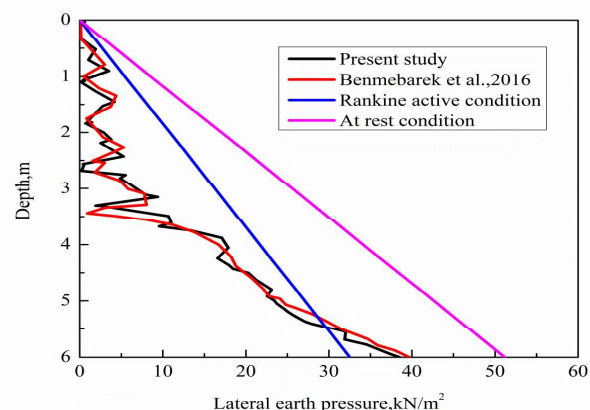
3.1 Lateral earth pressure distribution

Lateral pressures at 4.2 m from the concrete block facing are taken for analysis. It was noted that the lateral stresses at the termination of the reinforced zone of BBMSEW are increasing with the depth of the wall. From validation, it showed a maximal difference of approximately 5%.

In this study, a typical W/H ratio of 2 and 1.4 of BBMSEW with unreinforced zone and different values of stiffness was analyzed. The model was vigorous considering staged construction. The lateral and vertical earth pressures at 4.2 m from facing (i.e., termination of the reinforced zone) and the tensile profiles were also studied and results are presented.

Fig.4. Lateral stress at 4.2m from facing for $W/H=2$

From Fig.4. It is noted that the lateral stresses for case 1. $W/H=2$, is close to Rankine's active condition and from the $1/4H$, the lateral stress exceeds the Rankine's active stress condition and reaches to At-rest condition, this is due to the toe impediment imposed at the base of BBMSEW. And the percentage error with the validated model is approximately 2.75% and is satisfactory with the FHWA design guideline when $W/H=2$.

Fig.5. Lateral stress at 4.2m from facing for $W/H=1.4$

From Fig.5. it is noticed that the lateral stress at the ending of the reinforced zone and after construction the lateral earth pressures are increasing with the depth and less than Rankine's active condition. Nevertheless, in the $1/4H$ where it tends to exceed Rankine active condition and reaches to At rest condition due to the fixed rigidity above the foundation on which the wall rests and within the concrete block facing as seen by the wall displacements. The percentage error of the validated model is approximately 2.94% and is compared well for $W/H=1.4$ and the stresses are not as per the design guidelines of FHWA.

3.2 Tension Forces across the wall height

The distribution of tensile force across the reinforcement length is analyzed and observed that the tensile forces distributed are not uniform which are mobilized in the soil. So at every stage, the maximum tension force is taken and plotted with the wall height at different reinforcement heights. The

locus of maximum tension points in the backfill is similar to the tieback wedge method for a single MSE wall.

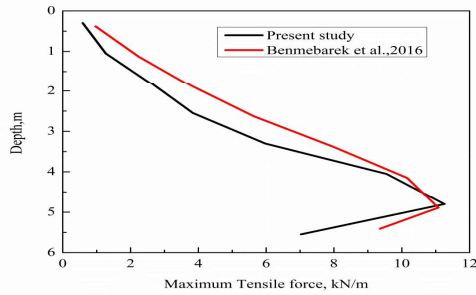


Fig.6. Maximum tension points profile for $W/H=2$.

Form Fig.6, for $W/H=2$ it is interpreted that the locus of maximum tension points is increasing with depth except for the $0.2H$ from the bottom of the wall where it is having the maximum tensile force and is compared well with the validated model.

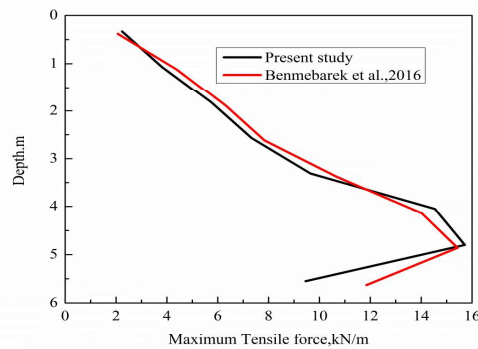


Fig.7. Maximum tension points profile for $W/H=1.4$.

From Fig.7, for $W/H=1.4$ it is noticed that the locus of maximum tension line increases with wall depth except for the wall height of $0.2H$ from the bottom and is compared well with a validated model with a maximal difference of approximately 4%.

4. Results

4.1 Lateral stress at the back of the reinforced zone

The lateral stress is taken at $4.2m$ from the concrete block facing i.e., at the termination of the reinforced zone along with wall height after construction is taken for the analysis, from Fig.8. It is observed that with a surcharge up to $\frac{1}{2}H$, the lateral stress is similar to the Rankine's active stress condition, and from $3m$ height, the lateral earth pressures are reducing linearly due to the arching phenomena in BBMSEW. And at $6m$ height the difference of earth pressure without surcharge is approximately 67.88% and with a surcharge from the Rankine's active condition was approximately 44.33%. The horizontal stress is increased with surcharge and at $6m$ it is increased approximately 42.31%. The reduction of lateral stress is due to the arching effect and with surcharge; the arching is more distinct with the stress analysis.

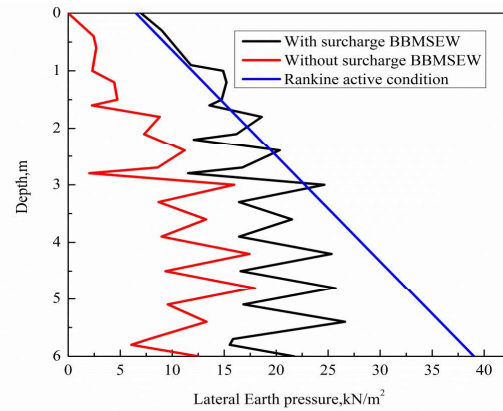


Fig.8. Comparison of lateral stress at the back of reinforced zone with surcharge.

4.2 Vertical stress at the termination of the reinforced zone

The lateral stresses are reduced due to the arching phenomena wherein which the vertical stress is the reason for the reduction and from the numerical analysis, it is spotted that vertical stresses are lesser than the overburden stress and there is stress redistribution behind the reinforced zone and this stress redistribution is due to stress transfer of the soil in the unreinforced zone on to the adjacent more rigid reinforced zone which is the effect of arching in the transition plane of reinforced and unreinforced zone. A new formula is derived for the stresses due to earth pressure considering the phenomena of arching in BBMSEW.

4.3 The equation for the stresses considering arching phenomena

The equation for vertical stress in the unreinforced zone of BBMSEW is derived from the equality of forces acting on the assumed unreinforced block considering arching, the schematic of the BBMSEW, and the forces acting is shown in Fig.9. And the FBD (force diagram) of the forces in the unreinforced block is shown in Fig.10.

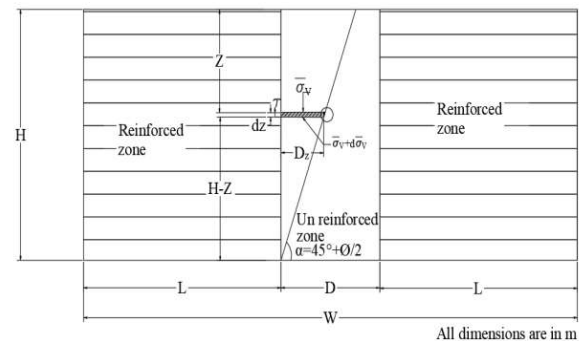


Fig.9. Schematic of BBMSEW for the derivation of vertical stress.

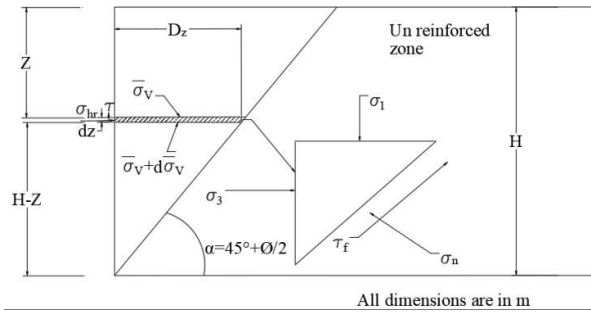


Fig.10. Free body diagram of unreinforced zone considered for the arching equation.

Equating all forces acting in a vertical direction on the rectangular element gives

The weight of a rectangular element,

$$dW = \gamma A dz \quad (1)$$

$$\text{shear load, } ds = (K\sigma_v \tan \delta + c_a) P dz \quad (2)$$

$$\text{From equilibrium, } d\sigma_v = \gamma \times dz - (K\sigma_v \tan \delta + c_a) \frac{P}{A} dz \quad (3)$$

Where P = perimeter of the element and A = c/s area of the element

$$\frac{d\sigma_v}{dz} = \left(\gamma - \frac{P}{A} c_a \right) - \left(K \tan \delta \frac{P}{A} \right) \sigma_v \quad (4)$$

$$\text{Let } X = \left(\gamma - \frac{P}{A} c_a \right); Y = \left(K \tan \delta \frac{P}{A} \right)$$

$$\frac{d\sigma_v}{dz} = X - Y \sigma_v$$

$$\frac{d\sigma_v}{X - Y \sigma_v} = dz$$

Integrating the above equation with the boundary condition for the vertical stress q to σ_v and at a depth z .

$$\int_q^{\sigma_v} \frac{d\sigma_v}{X - Y \sigma_v} = \int_0^z dz$$

The general equation for average vertical stress

$$\sigma_v = \frac{\left(\gamma - \frac{P}{A} c_a \right)}{\left(K \tan \delta \frac{P}{A} \right)} \left(1 - e^{-K \tan \delta \frac{P}{A} z} \right) + q e^{-K \tan \delta \frac{P}{A} z} \quad (5)$$

when the backfill is granular and there is a narrow trench, $L \gg B$,

$$\left(\frac{P}{A} \right) = \frac{2(B+L)}{BL} \text{ i.e., } \left(\frac{P}{A} \right) = \frac{2}{B}$$

$$\sigma_v = \left(\frac{\gamma B}{2K \tan \delta} \right) \left(1 - e^{-K \tan \delta \left(\frac{2}{B} \right) z} \right) + q e^{-K \tan \delta \left(\frac{2}{B} \right) z} \quad (6)$$

When there is no surcharge,

$$\sigma_v = \left(\frac{\gamma B}{2K \tan \delta} \right) \left(1 - e^{-K \tan \delta \left(\frac{2}{B} \right) z} \right) \quad (7)$$

Where, σ_v = average vertical stress; k = lateral earth pressure coefficient; and B = width of unreinforced zone; δ = fill-wall interfacial friction angle; z = depth of wall. The analytical equation derived for the BBMSE wall is compared with the numerical analysis values obtained from Plaxis 2D and the plots are presented in the paper.

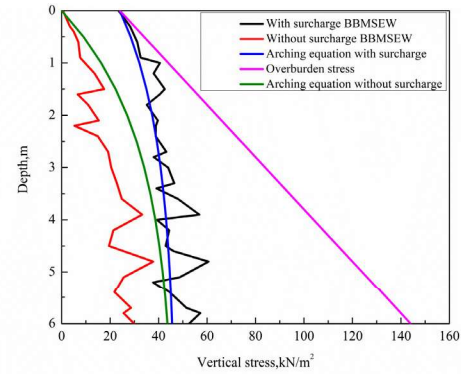


Fig.11. Vertical stress and arching equation comparison with and without surcharge.

From Fig.11, it is noticed that the vertical stresses are lower in value than overburden stress and follow the similar trend of the equation derived for vertical stress considering arching. It is due to the stress redistribution at the transition zone of the reinforced and unreinforced zone. Two cases are considered with surcharge and without surcharge for both analytical arching equation and the numerical analysis. From the plots after construction and at the termination of the reinforced region the vertical stress increases linearly with depth but is lower in value than overburden stress due to the arching.

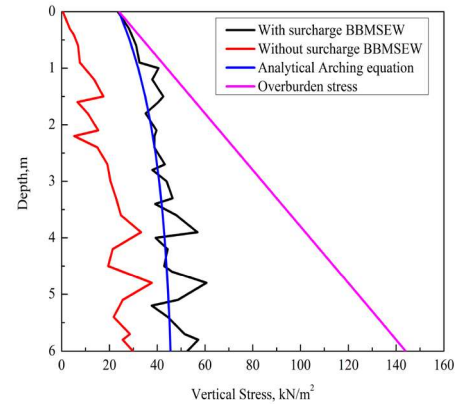


Fig.12. Vertical stresses with and without surcharge comparison with the analytical arching equation

when the case with surcharge is taken from the numerical analysis from Fig 12. It is noted that results of vertical stress nearly fall on the analytical arching equation derived for a surcharge and is nearly 63.51% less than the overburden pressure.

When the case without surcharge is considered the vertical stress from the numerical analysis is slightly less than the analytical arching equation and follow the similar trend of the arching equation without surcharge and is approximately 79.22% less than the overburden pressure after construction of the wall and at the end of the reinforced zone of BBMSEW. It shows that the arching is predominant in BBMSEW and is comparatively more in the case of the wall without surcharge. In the case of surcharge, the degradation of arching has happened in the transition plane of the reinforced and unreinforced region of the wall due to the additional vertical stress as a consequence of the surcharge on the wall. From Fig.12, the numerical analysis of the case with and without surcharge the vertical stresses with a surcharge is increased about 43.08% to that of the case without a surcharge after construction. And it is noted that the arching is more in the case of the wall without surcharge whereas in the case of the wall with a surcharge due to the additional vertical stresses comparatively the arching is less than the case without surcharge.

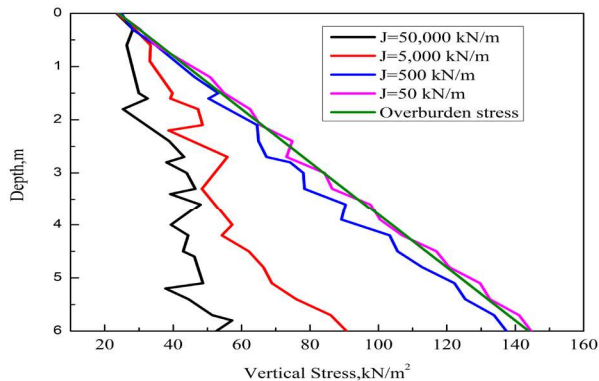


Fig.13. Vertical stresses at the back of reinforced zone for various stiffness.

To understand the realistic behavior of arching in the transition plane from the numerical analysis the stiffness of reinforcement ranging from $J=50,000$ kN/m to $J=50$ kN/m is considered and it is interpreted from Fig.13, that with the rise in stiffness there is more rigidity in the reinforced zone which increases the arching and it is observed that for the less stiffness the vertical stress is nearly overburden stress which shows that there is a negligible effect of arching in the transition plane and also the negligible effect of reinforcement is noticed. And with the increase in the stiffness of reinforcement the vertical stress is reduced nearly 63.50% to that of the overburden stress, this is due to more stress redistribution in the case of the more rigid reinforced zone and the arching is more.

From Fig.14, it is observed that the lateral displacements are tending outward more in case of the backfill reinforced with the stiffness of $J=50$ kN/m and less or reduced lateral displacements are observed within the reinforced zone with the stiffness of $J=50,000$ kN/m and when the surcharge is applied on the top of the BBMSEW. This less stiffness of reinforcement tends the wall to move away which causes lateral bulging showing the negligible effect of reinforcement compared to the case with higher stiffness.

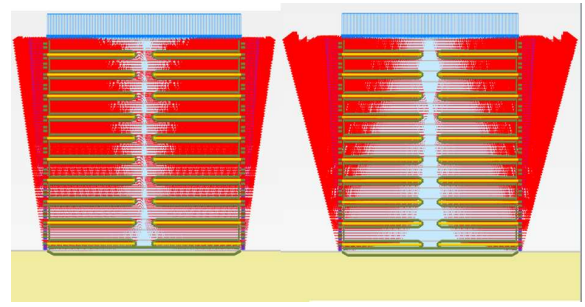


Fig.14. Variation of lateral displacement contours in $J= 50000$ and $J=50\text{kN/m}$

4.4 Surface settlement profiles

As represented in Fig.15. The settlements are more in the unreinforced zone. As it is obvious that the less rigidity zone will have more settlement compared to the rigid reinforced zone. As there is a rigidity difference between the reinforced and unreinforced zone of BBMSEW there is stress transfer between these zones and leads to arching phenomena in BBMSEW. And also the arching in the unreinforced zone will happen when the reinforced zone is rigid enough whereas in the case of the reinforcement rigidity is less as observed the settlements are transferred to the reinforced zone in which the reinforcement effect is negligible in case of reinforcement with the stiffness of $J=50$ kN/m. but when the reinforced zone is more rigid i.e., with reinforcement stiffness of $J=50,000$ kN/m, the settlements are observed in the unreinforced zone.

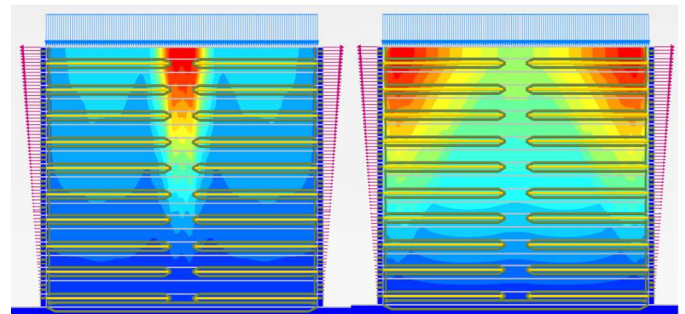


Fig.15. Settlement variation in BBMSEW for $J=50000$ and $J=50\text{kN/m}$

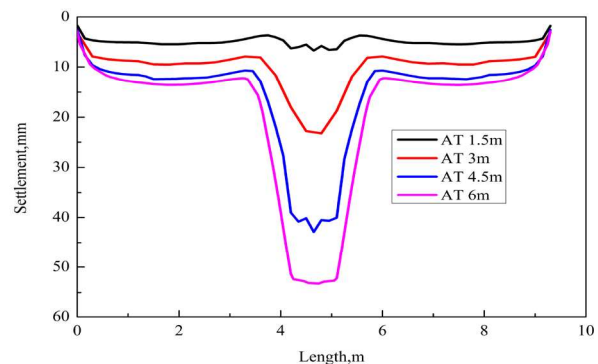


Fig.16. Surface settlement profiles at different depths for particular stiffness of $J=50000\text{kN/m}$.

It is observed from Fig.16, for particular reinforcement stiffness of $J=50000$ kN/m, for different heights of the wall after construction the surface settlement with surcharge is more compared to without surcharge. The different wall heights taken are 1.5 m, 3 m, 4.5 m, and 6 m, it is found that the unreinforced zone settled more than the reinforced zone due to the more rigidity of the reinforced zone and it leads to the differential settlement which directly leads to the arching in the transition zone of the reinforced and unreinforced zone. This arching action takes place due to the difference in stiffness between the reinforced and unreinforced region of the backfill. The average settlement of reinforced zone for 1.5 m, 3 m, 4.5 m, and 6 m height of the wall are respectively 4.82 mm, 8.91 mm, 12.82 mm, and 15.39 mm and in the unreinforced zone, the average settlement for the same heights of the wall are respectively 6.20 mm, 21.56 mm, 40.85 mm and 52.81 mm. It is concluded that the surface settlement profiles are increasing with wall height in the reinforced and unreinforced zone of the BBMSEW. Due to the surcharge, there is more settlement which increases the relative stiffness between the reinforced and unreinforced zone and leads to arching and reducing the vertical stress.

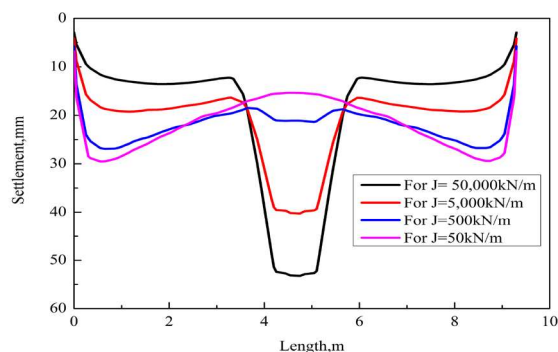


Fig.17. Surface settlement profiles after construction for various stiffness.

It is observed from Fig.17, that for a particular height after construction for various stiffness the surface settlement for reinforcement stiffness of $J=50$ kN/m, 500 kN/m, 5000 kN/m, and 50,000 kN/m in the reinforced zone are 22.32 mm, 22.02 mm, 18.85 mm, and 15.39 mm respectively. and for the same stiffness, the average settlement in the unreinforced zone is 15.45 mm, 21.16 mm, 39.81 mm, and 52.81 mm. It is found that for $J=50$ and 500 kN/m the settlements are more in the reinforced zone than the reinforced zone due to the less rigidity of the reinforcement the settlements are occurred in the reinforced zone, whereas for the stiffness of $J=5000$ and 50000 kN/m, it is found that the settlements are more in the unreinforced zone than the reinforced zone and with increment, in stiffness, there is a reduction in the settlement in the reinforced zone but more settlement has been observed in the unreinforced zone. It is concluded that for lesser stiffness there is the negligible effect of arching as the settlements are occurred in the reinforced zone due to less rigidity, with the increase in stiffness there is more rigidity due to this more relative stiffness between reinforced and unreinforced zone for which the arching is more predominant.

The incremental shear strain contours are shown in Fig.18, which are used for the determination of the critical failure mechanism of BBMSEW with varying reinforcement of $J=50$ kN/m and $J=50000$ kN/m.

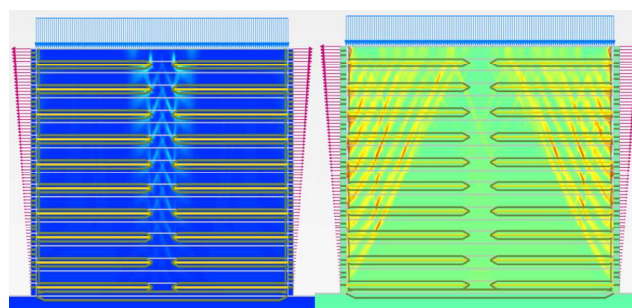


Fig.18. Incremental shear strain contours in BBMSEW for ($J=50000$ and $J=50$ kN/m).

In the case of high stiffness for $J=50,000$ kN/m, the interception of shear strain contours is formed like a triangular pattern observed in the unreinforced zone of BBMSE walls. But, in the case of less stiffness for $J=50$ kN/m, the shear strain contours are raised from the toe of the wall on both sides, as represented and follows the similar criteria of assumed failure plane as per FHWA guidelines. And also there is no effect of reinforcement as discussed earlier in the present study; this is due to more deformations in the less stiffness reinforcement as it is having the negligible effect of reinforcement in the reinforced zone of BBMSEW. These shear strain contours which are more often used to predict the failure mechanism of the BBMSEW.

5. Conclusions

In this study numerical analysis is done for the BBMSEW considering the typical W/H ratio of 1.55 and for this, the arching phenomena are analyzed, and the considerable outcomes of the study are pointed out below.

1. The lateral stresses with depth at the termination of the reinforced zone are increasing linearly but less than the Rankine active condition. For the ratio of width to height = 1.55, the horizontal stresses are reduced by about 44.33% to that of Rankine's active stress condition after construction.
2. The vertical stress nearly falls on the analytical arching equation derived for a surcharge and is nearly 63.51% less than the overburden pressure and the case without surcharge is approximately 79.22% less than the overburden pressure after construction, it replicates that on the application of surcharge the arching effect is more.
3. The vertical stress variation with surcharge applied on the top of BBMSEW with the increase in stiffness ($J=50000$ kN/m) the vertical stresses are reduced nearly 63.50% to that of overburden pressure whereas in the case of reinforcement stiffness ($J=50$ kN/m) the vertical stresses are similar to the overburden stress. It shows a negligible effect of arching as there is no rigidity difference between reinforced and unreinforced zone for the reinforcement stiffness of ($J=50$ kN/m).
4. The variation of settlement profiles for a particular stiffness with surcharge is non-uniform along the length of the reinforcement, but it is increasing with wall height in both reinforced and unreinforced zone and it is more in the unreinforced zone.
5. The variation of surface settlement at the end of construction for various stiffness is non-uniform across the entire length of reinforcement and it is observed that for lesser stiffness there is a negligible effect of arching as the settlements are occurred in the reinforced zone due to less rigidity, with the increase in stiffness there is more rigidity, and the arching effect is predominant.

References

- [1] A. A. of S. H. and T. O. ASHTO, *AASHTO LRFD Bridge Design Specifications*, Washington, DC, 2012.
- [2] M. Adams, J. Nicks, T. Stabile, J. Wu, W. Schlatter, and J. Hartmann, "Geosynthetic Reinforced Soil Integrated Bridge System, Synthesis Report", no. Publication no. FHWA-HRT-11-027, p. 64, 2011, [Online]. Available: <https://www.fhwa.dot.gov/publications/research/infrastructure/structures/11027/11027.pdf>.
- [3] R. L. Carter and M. Bernardi, "NCMA's design manual for segmental retaining walls," *Geosynthetics*, vol. 32, no. 1, 2014.
- [4] IRC:SP:102, "Guidelines for design and construction of reinforced soil walls," *Indian Roads Congr. New Delhi*, 2014.
- [5] "BS 8006-1:2010," *BS 8006-2010*, no. ISBN 978 0 580 53842 1, 2010.
- [6] R. H. B. Dov Leshchinsky, "GEOSYNTHETIC REINFORCED SOIL STRUCTURES," *J. Geotech. Eng.*, vol. 115, no. 10, pp. 1459–1478, 1990.
- [7] Steward et al, "GUIDELINES FOR THE DESIGN OF FLEXIBLE PAVEMENTS FOR LOW VOLUME RURAL ROADS," 2015.
- [8] J. Han and D. Leshchinsky, "Analysis of back-to-back mechanically stabilized earth walls," *Geotext. Geomembranes*, vol. 28, no. 3, pp. 262–267, 2010, doi: 10.1016/j.geotextmem.2009.09.012.
- [9] R. El-Sherbiny, E. Ibrahim, and A. Salem, "Stability of Back-to-Back Mechanically Stabilized Earth Walls," no. li, pp. 555–565, 2013, doi: 10.1061/9780784412787.058.
- [10] M. Djabri and S. Benmebarek, "FEM Analysis of Back-to-Back Geosynthetic-Reinforced Soil Retaining Walls," *Int. J. Geosynth. Gr. Eng.*, pp. 1–8, 2016, doi: 10.1007/s40891-016-0067-1.
- [11] S. Benmebarek, S. Attallaoui, and N. Benmebarek, "Interaction analysis of back-to-back mechanically stabilized earth walls," *J. Rock Mech. Geotech. Eng.*, vol. 8, no. 5, pp. 697–702, 2016, doi: 10.1016/j.jrmge.2016.05.005.
- [12] S. Benmebarek and M. Djabri, "FEM to investigate the effect of overlapping-reinforcement on the performance of back-to-back embankment bridge approaches under self-weight," *Transp. Geotech.*, vol. 11, pp. 17–26, Jun. 2017, doi: 10.1016/J.TRGEO.2017.03.002.
- [13] G. Rajagopal and S. Thiyyakkandi, "Numerical evaluation of the performance of back-to-back MSE walls with hybrid select-marginal fill zones," *Transp. Geotech.*, vol. 26, p. 100445, 2021, doi: 10.1016/j.trgeo.2020.100445.
- [14] S. M. Sravanam, U. Balunaini, and R. M. Madhira, "Behavior of Connected and Unconnected Back-to-Back Walls for Bridge Approaches," *Int. J. Geomech.*, vol. 20, no. 7, p. 06020013, 2020, doi: 10.1061/(asce)gm.1943-5622.0001692.
- [15] A. Palat, "Settlement Analysis of Unreinforced and Reinforced Retaining Walls," in *International Conference on GEOTECHNIQUES FOR INFRASTRUCTURE PROJECTS*, 2018, no. February 2017.
- [16] S. H. Lajevardi, K. Malekmohammadi, and D. Dias, "Numerical Study of the Behavior of Back-to-Back Mechanically Stabilized Earth Walls," *Geotechnics*, vol. 1, no. 1, pp. 18–37, 2021, doi: 10.3390/geotechnics1010002.
- [17] U. Balunaini, S. M. Sravanam, and M. R. Madhav, "Effect of compaction stresses on performance of back-to-back retaining walls," *ICSMGE 2017 - 19th Int. Conf. Soil Mech. Geotech. Eng.*, vol. 2017-Sept, no. 1, pp. 1951–1954, 2017.
- [18] K. Hatami and R. J. Bathurst, "Development and verification of a numerical model for the analysis of geosynthetic-reinforced soil segmental walls under working stress conditions," *Can. Geotech. J.*, vol. 42, no. 4, pp. 1066–1085, 2005, doi: 10.1139/t05-040.
- [19] E. Guler, M. Hamderi, and M. M. Demirkan, "Numerical analysis of reinforced soil-retaining wall structures with cohesive and granular backfills," *Geosynth. Int.*, vol. 14, no. 6, pp. 330–345, 2007, doi: 10.1680/gein.2007.14.6.330.
- [20] H. Hashimoto, "FINITE ELEMENT STUDY OF A GEOSYNTHETIC REINFORCED SOIL RETAINING WALL WITH CONCRETE BLOCK FACING," vol. 7, no. 2, pp. 137–162, 2000.
- [21] C. S. Yoo and A. R. Song, "Effect of foundation yielding on performance of two-tier geosynthetic-reinforced segmental retaining walls: A numerical investigation," *Geosynth. Int.*, vol. 13, no. 5, pp. 181–194, 2006, doi: 10.1680/gein.2006.13.5.181.
- [22] S. H. Mirmoradi and M. Ehrlich, "Modeling of the compaction-induced stress on reinforced soil walls," *Geotext. Geomembranes*, vol. 43, no. 1, pp. 82–88, 2015, doi: 10.1016/j.geotextmem.2014.11.001.
- [23] B. Huang, R. J. Bathurst, K. Hatami, and T. M. Allen, "Influence of toe restraint on reinforced soil segmental walls," *Can. Geotech. J.*, vol. 47, no. 8, pp. 885–904, 2010, doi: 10.1139/T10-002.
- [24] M. S. Won and Y. S. Kim, "Internal deformation behavior of geosynthetic-reinforced soil walls," *Geotext. Geomembranes*, vol. 25, no. 1, pp. 10–22, 2007, doi: 10.1016/j.geotextmem.2006.10.001.
- [25] B. Huang, R. J. Bathurst, and K. Hatami, "Numerical Study of Reinforced Soil Segmental Walls Using Three Different Constitutive Soil Models," *J. Geotech. Geoenvironmental Eng.*, vol. 135, no. 10, pp. 1486–1498, 2009, doi: 10.1061/(asce)gt.1943-5606.0000092.
- [26] R. Karpurapu and R. J. Bathurst, "Behaviour of geosynthetic reinforced soil retaining walls using the finite element method," *Comput. Geotech.*, vol. 17, no. 3, pp. 279–299, 1995, doi: 10.1016/0266-352X(95)99214-C.
- [27] A. M. Belal and K. P. George, "Finite Element Analysis of Reinforced Soil Retaining Walls Subjected To Seismic Loading," *12Wcee*, no. 1, pp. 1–8, 2000.
- [28] J. T. Laba and J. B. Kennedy, "Reinforced Earth Retaining Wall Analysis and Design," *Can. Geotech. J.*, vol. 23, no. 3, pp. 317–326, 1986, doi: 10.1139/t86-045.
- [29] T. M. Allen, R. J. Bathurst, and R. R. Berg, *Global level of safety and performance of geosynthetic walls: An historical perspective*, vol. 9, no. 5–6, 2002.
- [30] S. H. Mirmoradi, M. Ehrlich, and C. Dieguez, "Evaluation of the combined effect of toe resistance and facing inclination on the behavior of GRS walls," *Geotext. Geomembranes*, 2016, doi: 10.1016/j.geotextmem.2015.12.003.
- [31] K. Hatami and R. J. Bathurst, "Numerical model for reinforced soil segmental walls under surcharge loading," *J. Geotech. Geoenvironmental Eng.*, vol. 132, no. 6, pp. 673–684, 2006, doi: 10.1061/(ASCE)1090-0241(2006)132:6(673).
- [32] A. Ghanbari et al., "Effect of Surcharge on Active Earth Pressure in Reinforced Retaining Walls: Application of Analytical Calculation on a Case Study To cite this version : HAL Id: hal-01717161," no. April, 2018, doi: 10.13140/RG.2.2.10335.36005.
- [33] H. Liu, "Reinforcement Load and Compression of Reinforced Soil Mass under Surcharge Loading," *J. Geotech. Geoenvironmental Eng.*, vol. 141, no. 6, p. 04015017, 2015, doi: 10.1061/(asce)gt.1943-5606.0001300.
- [34] B. Lien, "Modeling Traffic and Construction Equipment Surcharges for Geotechnical Analysis: 2-D or 3-D? □ Make a Complicated Question Simple ... □ Make a Simple Question

Complicated ... What is the Typical Highway Live / Traffic Surcharge Load in Geotechnical Desig,” pp. 1–12, 2017.

[35] C. Yoo and S. Bin Kim, “Performance of a two-tier geosynthetic reinforced segmental retaining wall under a surcharge load: Full-scale load test and 3D finite element analysis,” *Geotext. Geomembranes*, vol. 26, no. 6, pp. 460–472, 2008, doi: 10.1016/j.geotexmem.2008.05.008.

[36] S. M. Sravanam, U. Balunaini, and M. R. Madhav, “Behavior and Design of Back-to-Back Walls Considering Compaction and Surcharge Loads,” *Int. J. Geosynth. Gr. Eng.*, vol. 5, no. 4, pp. 1–17, 2019, doi: 10.1007/s40891-019-0180-z.

[37] P. Rajeev, P. R. Sumanasekera, and N. Sivakugan, “Average Vertical Stresses in Underground Mine Stopes Filled with Granular Backfills,” *Geotech. Geol. Eng.*, vol. 34, no. 6, pp. 2053–2061, 2016, doi: 10.1007/s10706-016-0082-y.

[38] N. Sivakugan and S. Widinghe, “Stresses Within Granular Materials Contained Between Vertical Walls,” *Indian Geotech. J.*, vol. 43, no. 1, pp. 30–38, 2013, doi: 10.1007/s40098-012-0029-z.

[39] A. Al-hassan, I. Katkhuda, and A. Barghouthi, “Narrow backfill lateral earth pressure,” *Arab Cent. Eng. Stud.*, pp. 1–10, 2009.

[40] W. A. Take and A. J. Valsangkar, “Earth pressures on unyielding retaining walls of narrow backfill width,” *Can. Geotech. J.*, vol. 38, no. 6, pp. 1220–1230, 2001, doi: 10.1139/cgj-38-6-1220.

[41] S. Widinghe and N. Sivakugan, “Vertical Stresses within Granular Materials in Silos,” no. 061, pp. 590–595, 2012.

[42] L. Miao, F. Wang, J. Han, and W. Lv, “Benefits of geosynthetic reinforcement in widening of embankments subjected to foundation differential settlement,” *Geosynth. Int.*, vol. 21, no. 5, pp. 321–332, 2014, doi: 10.1680/gein.14.00019.

[43] T. Hsien-Jen, “A Literature Study of the Arching Effect,” *Thesis Res.*, no. February, pp. 1–196, 1996.

[44] S. Shukla and N. Sivakugan, “A simplified extension of the conventional theory A simplified extension of the conventional theory of arching in soils,” vol. 6362, no. March, 2016, doi: 10.3328/IJGE.2009.03.03.353-359.

[45] K. Pirapakaran and N. Sivakugan, “Arching within hydraulic fill stopes,” *Geotech. Geol. Eng.*, vol. 25, no. 1, pp. 25–35, 2007, doi: 10.1007/s10706-006-0003-6.

[46] R. S. Dalvi and P. J. Pise, “Effect of arching on passive earth

pressure coefficient,” *12th Int. Conf. Comput. Methods Adv. Geomech. 2008*, vol. 1, pp. 236–243, 2008.

[47] K. H. Paik and R. Salgado, “Estimation of active earth pressure against rigid retaining walls considering arching effects,” 2003.

[48] S. Singh, S. K. Shukla, and N. Sivakugan, “Arching in Inclined and Vertical Mine Stopes,” *Geotech. Geol. Eng.*, vol. 29, no. 5, pp. 685–693, 2011, doi: 10.1007/s10706-011-9410-4.

[49] P. P. Dalvi RS, “Effect of arching on passive earth pressure coefficient,” in *Proceedings of 12th IACMAG conference*, 2018, pp. 236–243.

[50] C. Thomas and J. Shiau, “common ground 07 Modelling the arching effect in active earth pressure problems,” no. Coduto, pp. 262–267, 1999.

[51] G. Moradi and A. Abbasnejad, “The State of the Art Report on Arching Effect,” *J. Civ. Eng. Res.*, vol. 3, no. 5, pp. 148–161, 2013, doi: 10.5923/j.jce.20130305.02.

[52] M. Liu, X. Chen, Z. Hu, and S. Liu, “Active earth pressure of limited $c-\phi$ soil based on improved soil arching effect,” *Appl. Sci.*, vol. 10, no. 9, 2020, doi: 10.3390/app10093243.

[53] C. G. Kellogg, “The arch in soil arching,” *J. Geotech. Eng.*, vol. 113, no. 3, pp. 269–271, 1987, doi: 10.1061/(ASCE)0733-9410(1987)113:3(269).

[54] A. Roy and N. R. Patra, “Effect of arching on passive earth pressure for rigid retaining walls considering translation mode,” *Proc. 2009 Struct. Congr. - Don't Mess with Struct. Eng. Expand. Our Role*, vol. 8, no. 2, pp. 2784–2793, 2009, doi: 10.1061/41031(341)304.

[55] P. Nagavalleswari and N. R. Patra, “Effect of Arching on Passive Earth Pressure for Rigid Retaining Walls Considering Rotation at Top,” *Int. J. Geomech.*, vol. 8, no. 2, pp. 123–133, 2017.

[56] M. A. Kumaar, S. Kommu, and S. S. Asadi, “Optimization of embankment widening with different soils,” *Int. J. Recent Technol. Eng.*, vol. 8, no. 3, pp. 711–715, Sep. 2019, doi: 10.35940/ijrte.C3971.098319.